J Surfact Deterg
DOI 10.1007/s11743-016-1816-9

ORIGINAL ARTICLE

# Phase Behavior of Ascorbyl Palmitate Coagels Loaded with Oligonucleotides as a New Carrier for Vaccine Adjuvants

**Gabriela V. Ullio Gamboa[1,2] · Luciano A. Benedini[3,4] · Pablo C. Schulz[3] · Daniel A. Allemandi[1,2]**

Received: 23 September 2015 / Accepted: 4 April 2016


**Abstract** In this work, the phase behavior variations of an ascorbyl palmitate ($Asc_{16}$) system in aqueous solution were analyzed when immunologically active hydrophilic compounds (CpG and OVA) were introduced. This study was carried out through optical polarizing microscopy (OPM) and differential scanning calorimetry (DSC) at different temperatures and over a broad range of concentrations. The combination of both techniques allowed the determination of a complete phase diagram which was compared with those built for $Asc_{16}$-water system and it was demonstrated that fixed concentrations of hydrophilic compounds (300 and 24 μg/g for CpG-ODN and OVA respectively) generate two lamellar liquid crystals, a cubic liquid crystal phase, and also other aggregates. However, no changes were observed in the phase diagram in terms of formation of new mesophases. The aqueous phase behavior was also studied as a function of surfactant and temperature. DSC and Fourier transform infrared spectroscopy (FT-IR) measurements show differences in the free water and mainly in the secondary hydration layer, which confirm that the studied compounds are situated in the aqueous domain. The construction and analysis of $Asc_{16}$ phase diagrams with a fixed concentration of CpG-ODN/OVA allows the comprehension of $Asc_{16}$ phase behavior and could be easily adapted to other concentrations. Moreover, these findings could be extrapolated to other hydrophilic substances in aqueous solution introduced in liquid crystal phases since they follow a similar behavior as those reported in the literature.

**Keywords** Ascorbyl palmitate · Liquid crystals · Oligonucleotides · Phase diagrams · Water behavior

## Introduction

Alkanoyl-6-*O*-ascorbic acid esters (Asc) help in the transfer of the antioxidant activity of vitamin C into lipophilic media. Due to their chemical structure i.e. a hydrophobic portion (hydrocarbon chain) and a polar group (ascorbic acid), these esters behave as amphiphilic molecules [1]. Furthermore, during the preparation of these chemicals the entire ascorbyl ring remains intact, therefore the final amphiphilic species undergo similar radical scavenging activity of vitamin C and the antioxidant efficacy is similar to others natural reducing compounds, for instance phenolic acids, flavonoids, and essential oils. Moreover, due to their structural architecture they can be easily solubilized in hydrophobic liquids, or mixed with biological lipophilic compounds such as fats, oils, vitamins, and lipid membrane bilayers [2].

Ascorbic acid esters form supramolecular aggregates in aqueous dispersions; their nature depends on their chemical structure, concentration, and temperature. The phase

Gabriela V. Ullio Gamboa and Luciano A. Benedini contributed equally to this work.

✉ Daniel A. Allemandi
dalemand@gmail.com

[1] Unidad de Investigación y Desarrollo en Tecnología Farmacéutica (UNITEFA-CONICET), 5000 HUA Córdoba, Argentina

[2] Departamento de Farmacia, Facultad de Ciencias Químicas, Universidad Nacional de Córdoba, 5000 HUA Córdoba, Argentina

[3] Departamento de Química, Universidad Nacional del Sur, 8000 Bahía Blanca, Argentina

[4] Instituto de Química del Sur (INQUISUR-CONICET), 8000 Bahía Blanca, Argentina

Published online: 26 April 2016

behavior of $Asc_n$ ($c_n$ being the length of the alkyl chain) is probably one of the most reliable physicochemical evidence of the complex series of intermolecular interactions (hydrophobic, electrostatic and hydrogen bonding interactions), which control the thermal behavior of aqueous dispersions of these surfactants. Ascorbyl palmitate ($Asc_{16}$) belongs to this family of molecules and its physicochemical behavior has been widely studied [1–4]. Ambrosi *et al.* [5] and later Benedini *et al.* [3] have reported that $Asc_{16}$-water system forms clear dispersions at temperatures higher than the critical micelle temperature (CMT) and at higher concentration than the critical micelle concentration (CMC). On cooling these water dispersions form coagels (Coa) [2, 6]. The "coagels" are hydrated crystalline phases [7–9] and their lamellar structure produces at least one highly ordered dimension, so they exhibit sharp X-ray diffraction (XRD) patterns and optical birefringence. Besides, they have been extensively studied as drug delivery systems with potential application in ocular and dermal therapies [9–11]. In this context, Benedini *et al.* [3] reported the complete phase diagram of $Asc_{16}$-water system in which, at concentration below to 0.48 weight fraction this system shows hydrated crystals in an isotropic liquid, and give rise to a lamellar liquid crystal when heated to $\sim$60 °C. Therefore, by mean of phase studies we were able to evaluate the potential utility of this new liquid crystal system, which has evidenced interesting properties as pharmaceutical carrier [2, 4, 12, 13].

Vaccine formulations are steering away from live attenuated microorganisms toward subunits of pathogens (highly purified or recombinant molecules). Although the latter antigens (Ag) are intrinsically safer, they are often poorly immunogenic as a result of the inadequate inherent immune-stimulatory property and therefore they require an adjuvant to trigger an efficient immune response. In immunology, the term "vaccine adjuvant" comprises all molecules/compounds or formulations that are able to stimulate the specific immune response when used in combination with Ag [14]. In that sense, there has been significant interest in the potential use of oligodeoxynucleotides (ODN) containing specific cytosine-guanine (CpG) sequences as an immunotherapy for malignant, infectious and allergic diseases [15, 16]. In contrast to currently licensed adjuvants, CpG-ODN have demonstrated that they elicit strong humoral and cellular immune responses towards a broad heterogeneity of Ag and confer protection against a wide variety of bacterial, viral, and parasitic agents in several animal models [17, 18].

The mechanisms of action which control the synergistic responses between CpG-ODN and Ag are not well understood, but numerous factors could contribute such as the protection of CpG-ODN from enzymatic degradation, a depot effect whereby CpG-ODN is gradually released from the site of injection, and possibly an increasing uptake by antigen presenting cells (APC) for example dendritic cells [19]. While preliminary human experimentation has yielded encouraging results, clinical use of free CpG-ODN still deal with different challenges, which limit their effectiveness. These comprise lack of *in vivo* stability, toxicity, unfavorable biodistribution/pharmacokinetic pattern, unspecificity for target cells and a weakly intracellular uptake [17, 20, 21]. In this context, the development of an efficient drug carrier system which could overcome these drawbacks and improve the adjuvant properties of CpG-ODN is mandatory. To this end, a great number of formulations have been explored, such as microspheres [22] liposomes [23] nanoparticles [24] and nanotubes [25] applying different material engineering and technological approaches. Although some of these formulations appeared promising, they also have had some problems mainly relating to manufacturing issues, such as scaling-up, toxicity associated with cationic materials, and the purity of the products [26, 27].

On the other hand, the formulation of CpG-ODN impact on the immune response, and therefore, the resulting therapeutic effects. It is expected that the efficacy of CpG-ODN could be substantially improved by using appropriate drug delivery systems. Early experiments showed that the addition of CpG-ODN to a conventional protein model Ag such as ovalbumin (OVA) boosts the antibody production by approximately threefold [28]. In those experiments, both OVA and CpG-ODN were free to diffuse from the site of injection.

Results from different investigations have reported that immunological activity is improved by linking CpG-ODN directly to the Ag, [29] co-encapsulating into liposome vesicles [23] or adsorbing them onto cationic poly-actide co-glycolides (PLG) microparticles [30]. Regarding this, conjugates containing CpG-ODN and Ag were preferably taken up by APC leading to significantly higher cytotoxic T lymphocytes responses compared to unconjugated mixtures. Such results confirm the hypothesis that optimal immunological response is achieved once Ag and adjuvant are presented to the immune system in temporal and spatial closeness. However, it is difficult to compare different formulations of CpG-ODN reported in the literature because the amount and the type of CpG-ODN/OVA as well as the mouse strain and the immunization protocols are divergent. For example, Erikci *et al.* [31] showed the results in Balb/c mice immunized with OVA (7.5 μg) and CpG-ODN (15 μg) co-encapsulated in anionic nanoliposomes injected intraperitoneally. Similarly, in Fischer *et al.* [32] experiments, one group of mice received 10 mg of chitosan-coated PLGA microparticles contained between 90 and 140 μg of OVA peptide (SIINFEKL) covalently attached to CpG-ODN (20 μg). There are almost endless

combinations of doses that are possible and doing such studies in mouse models just contribute to estimate the optimal human dose for CpG-ODN since the activity in humans may be less than in mice, due to differences in TLR9 expression in dendritic cell populations [33].

Accordingly, CpG-ODN was formulated with OVA in coagels formed by self-assembly of Asc16 [34]. Here, the authors showed that CpG-ODN loaded into Coa-Asc16 dramatically enhances the magnitude of both OVA-specific humoral (immunoglobulins G1 and G2) and cellular (interferon gamma and interleukin 17) immune responses even when the dose of CpG-ODN was reduced twice compared to CpG-ODN in solution. Sanchez Vallecillo *et al*. [34] hypothesized that the particular local immunocompetent environment created by coagels may significantly impact in the final OVA-specific immune response. This could be one of the mechanisms by which coagels increases the immunogenicity of OVA/CpG-ODN.

Even if several structure and dynamics features of bulk water could be considered as rational, these could not be applied to water found in interfacial or restricted environments. Therefore, the activity of water molecules could be restricted when they are linked to the protein's surface, lyotropic liquid crystals or micelles. The water layer in the pool of a reverse micelle is heterogeneous, even on a molecular level, and its properties in the layer are susceptible to the detailed interactions with the adjacent surface [35]. The water in the immediacy of biomolecules, e.g., biological water is especially relevant to their organic or living functions. Furthermore, biological macromolecules are physiologically inactive in the absence of water. In regards to this, the properties of water in colloidal systems represent a significant factor that must be considered [5].

In summary, the analysis of the physicochemical behavior of systems based on lamellar structures such as coagels could lead to elucidate the mechanisms that govern the establishment and the way of action of CpG-ODN once incorporated into this carrier. Another important aspect for systems that are likely to be applied for biological processes is the function of water found in the polar layer. Regarding this, the conformation and dynamics of water in the microstructure of aqueous surfactants represent an essential point in the comprehension of the aggregation phenomena and the resulting interactions in the inner phase. Taking into account these considerations, the aim of this work was to study the whole phase diagram of the CpG-ODN/$Asc_{16}$-dextrose solution in order to evaluate the modification in the structure of $Asc_{16}$ in solution induced by CpG-ODN and thus, the change in the water behavior in these supramolecular structures. The characterization of nature of the phases and water behavior into bilayers was performed by differential scanning calorimetry (DSC) and the observation of textures through an optical polarizing microscope (OPM) at different concentrations and temperatures. The results of water behavior were confirmed by Fourier transform infrared spectroscopy (FT-IR). Finally, the results were compared with those obtained by Benedini *et al*. [3] in which a complete phase diagram for $Asc_{16}$-water system was described (Fig. 1).

## Materials and Methods

### Materials

Phosphorothioated CpG oligodeoxynucleotide 1826, seq (5′–3′: tccatgacgttcctgacgtt) was acquired from Operon Technologies Inc. (Alameda, California, USA) and it was reconstituted in 0.9 % NaCl saline solution (B. Braun Medical S.A, Buenos Aires, Argentina) to a final concentration of 1 mg/ml. Ovalbumin (albumin from chicken egg white grade v A5503) was purchased from Worthington Biochemical (New Jersey, USA) and OVA stock solution was prepared in dextrose 5 % solution (Roux-Ocefa Buenos Aires, Argentina) to reach a 10 mg/ml final concentration. L-ascorbic acid 6-hexadecanoate ($Asc_{16}$) was obtained from Fluka Analytical (Saint Quentin Fallovier, France). All others chemicals were of analytical grade and used as received.

### Methods

The samples were prepared by mixing the components ($Asc_{16}$, dextrose solution, and CpG-ODN/OVA) in the chosen ratios in glass containers. The suspensions were heated (72 °C) in ultrasonic equipment (15 min), left to reach room temperature in hermetically sealed plastic tubes and kept in darkness for further analyses. The dispersions were made with an increasing concentration (C) of $Asc_{16}$: 0.02, 0.05, 0.10, 0.3, 0.5 and 0.7 weight fraction in dextrose solution. Equivalent samples were prepared by replacing the dextrose solution with 75 and 6 µl of CpG-ODN and OVA solutions respectively in order to obtain the loaded systems while maintaining the concentration of $Asc_{16}$ constant. These quantities were the same as those used in the *in vivo* experiments developed by Vallecillo *et al*. [34] and were kept constant in all samples. Mouse strains and adjuvant doses for this model antigen were determined to be optimal based on previous studies conducted in our laboratories [36, 37].

Special attention was paid to reduce $Asc_{16}$ oxidation by dissolved oxygen taking rigorous care to minimize the contact with air [38, 39]. Considering the possible

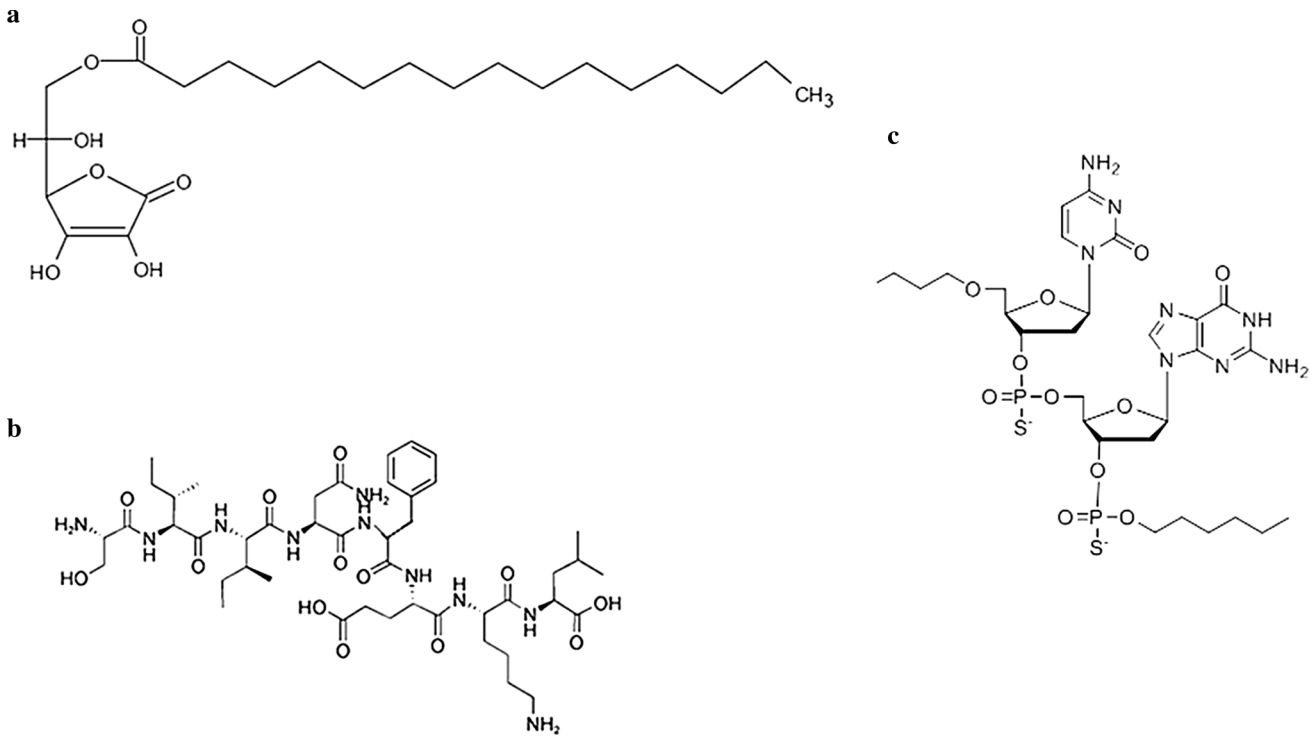


**Fig. 1** Chemical structures. **a** Ascorbyl palmitate ($Asc_{16}$). **b** Ovoalbumine (OVA). **c** Oligodeoxynucleotides with CpG motifs (CpG-ODN)

oxidation of the cyclic ring, the length of degraded Asc16 in lamellar mesophases and crystals is predicted to be further diminished in these micro-environments due to the low water exposition. In addition, the confinement of water in the lamellae reduces the possibility of oxygen diffusion inside the crystalline and liquid crystalline microstructures.

### Differential Scanning Calorimetry Measurements (DSC)

Calorimetric measurements were performed with a Q20 Differential Scanning Calorimeter (TA Instruments). Samples were prepared using hermetically sealed aluminium pans which had been weighed with a ±0.00001 g precision balance. The samples were previously cooled to 20 °C for 5 min (min). Afterwards they were heated up to 150 °C at a rate of 5 °C/min. Occasionally, several samples were maintained at this temperature for 1 min in order to corroborate the decomposition of $Asc_{16}$ revealed by changes in the heat flow. No degradation was detected under these conditions (samples in hermetically sealed pans at 120 °C). Others dispersions were also cooled at the same ratio and the cycle was carried out again. Under these new conditions, no significantly changes in comparison with the first cycle were observed. The superposed peaks were analyzed by means of Gaussian fits and the phase diagram obtained displayed contrasting regions delimited by the transition temperatures.

### Optical Polarized Microscopy (OPM)

A polarizing microscope (Nikon Eclipse E-200 POL, Tokyo, Japan) was used for optical microscopy analyses. The microphotographs were taken from dispersions placed within glass slides and heated in order to achieve one of the distinctive areas present in the phase diagram defined by calorimetric analyses. Aiming to determine the various phase changes, the textures observed on cooling were also recorded. Additionally, images were recorded with a lambda ($\lambda$) retardation plate and without crossed polarizers.

### Infrared Spectroscopy (FT-IR)

A full scanning spectrum (64 scans) ranged from 4000 to 400 $cm^{-1}$ was obtained on a Thermo Nicolet FT-IR-Nexus 470 equipped with a Nichrome DTGS Detector and a KBr beamsplitter (Minnesota, USA). The background was established with anhydrous KBr. Log mode: as a solid dispersion in a solid (2.0 mg of anhydrous compound in 150 mg of anhydrous KBr) contained in a microcapsule Diffuse Reflectance accessory.

### Water Properties

The determination of water properties and the number of water molecules per molecule of $Asc_{16}$ was carried out by means of DSC, FT-IR and thermodynamic calculations.

### Phase Diagram

The identification of the nature of the diverse phases was carried out by observation of the optical textures at different concentrations and temperatures using polarized microscopy and comparing the results with those obtained by DSC and thermodynamic calculations. Once thermograms have been obtained, the heated plate of the microscope was set to the transitional temperatures that were observed in the thermograms and thus mesophases were imaged.

## Results and Discussion

### DSC Determinations of Water Properties in CpG-ODN/OVA/$Asc_{16}$-Dextrose Solution

Since water content modifies the structure of $Asc_{16}$ coagels, a description of phase behavior is presented in this section. Figure 2 shows the thermograms of the following systems: $Asc_{16}$-water, $Asc_{16}$-dextrose solution, CpG-ODN/$Asc_{16}$-dextrose solution and CpG-ODN/OVA/$Asc_{16}$-dextrose solution. It should be noted that the transition points of water and $Asc_{16}$ for the last system do not show any variation compared to the $Asc_{16}$-water system. Therefore, neither the presence of CpG-ODN nor OVA alter the transition temperatures of the $Asc_{16}$-water system. The comparison of DSC thermograms of $Asc_{16}$-dextrose solution and $Asc_{16}$-water systems shows that there are no considerable differences between them. This fact allows us to suggest that the structuring effect of dextrose does not substantially change the appearance and the number of phases found in the $Asc_{16}$-water system.

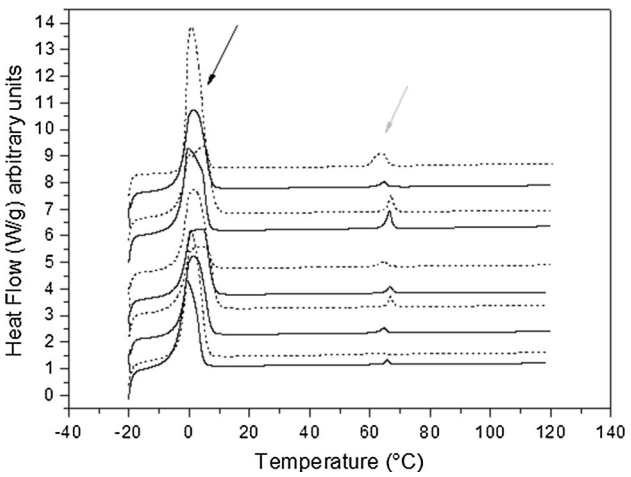


**Fig. 2** Thermograms of $Asc_{16}$ solutions (Heat flow *vs* temperature). Samples composition from the top to the bottom: CpG-ODN/$Asc_{16}$ 0.05 weight fraction in dextrose solution, CpG-ODN/OVA/$Asc_{16}$ 0.1 weight fraction in dextrose solution, $Asc_{16}$ 0.1 weight fraction in water, CpG-ODN/$Asc_{16}$ 0.05 weight fraction in dextrose solution, CpG-ODN/OVA/$Asc_{16}$ 0.05 weight fraction in dextrose solution, $Asc_{16}$ 0.1 weight fraction in dextrose solution, $Asc_{16}$ 0.02 weight fraction in dextrose solution, CpG-ODN/$Asc_{16}$ 0.02 weight fraction in dextrose solution, CpG-ODN/OVA/$Asc_{16}$ 0.02 weight fraction in dextrose solution, $Asc_{16}$ 0.05 weight fraction in dextrose solution. The *black arrow* indicates water transitions and the *grey arrow* indicates $Asc_{16}$ transitions

Regarding the effects induced by saccharides, Lo Nostro *et al.* [40] demonstrated that sucrose strengthens the hydrogen bonding network so that a higher temperature is essential to permit the breakdown of the lamellar coagel structure and the generation of a liquid micellar phase. Therefore, the authors also confirmed that a hydrogen bonding network in the bulk dissolvent is the determining point in the transition coagel/gel phase. However, in the present case the amount of dextrose was not high enough to modify the phase behavior. Therefore, we assume that the phase diagram built for the $Asc_{16}$-water system could account also for this system [3]. Furthermore, the lack of alterations of these transition temperatures in all the concentrations evaluated for this new system could be due to the low amounts of CpG-ODN and OVA in the samples.

Several investigations were conducted in order to understand the behavior of water in the interlayer space and the presence of different kinds of water which are affected by the surface of polar head groups of $Asc_{16}$. Therefore, as it was reported by Benedini *et al.* [3] for $Asc_{16}$-water system, three kinds of water could be detected. However, for $Asc_{16}$-dextrose solution loaded with CpG-ODN/OVA, the structure of the second hydration layer was considerably modified compared to $Asc_{16}$-water system (Fig. 3a).

As mentioned above, the superposed peaks of thermograms were analyzed by means of Gaussian fits and this makes it possible to assign to each water peak a single category. Thus, two kinds of water are perfectly distinguishable from the thermograms. The kind of water that starts to melt at 0 °C is bulk water; but there is other kind that starts to melt a few degrees before which is considered surface water. This kind of water is ascribed to a secondary hydration water layer. The number of molecules that belong to each of these layers is shown in Fig. 3a.

In $Asc_{16}$-water system, Benedini *et al.* [3] have demonstrated by DSC that there are three kinds of water: bulk water, second hydration layer and first hydration layer. The first hydration layer is identified by plotting the enthalpy *vs* sample concentration (Fig. 3b), and it is distinguished by the lack of melting peaks of water (Fig. 3c). In the first hydration layer the molecules of water are firmly linked to the polar heads groups of $Asc_{16}$ and do not freeze; and in consequence, they are not detected by DSC [41]. The overall water fusion peak disappeared at a $C = 0.55 \pm 0.005$ weight fraction (Fig. 3c). Therefore, there is no free water detectable, and thus, in Fig. 3b when

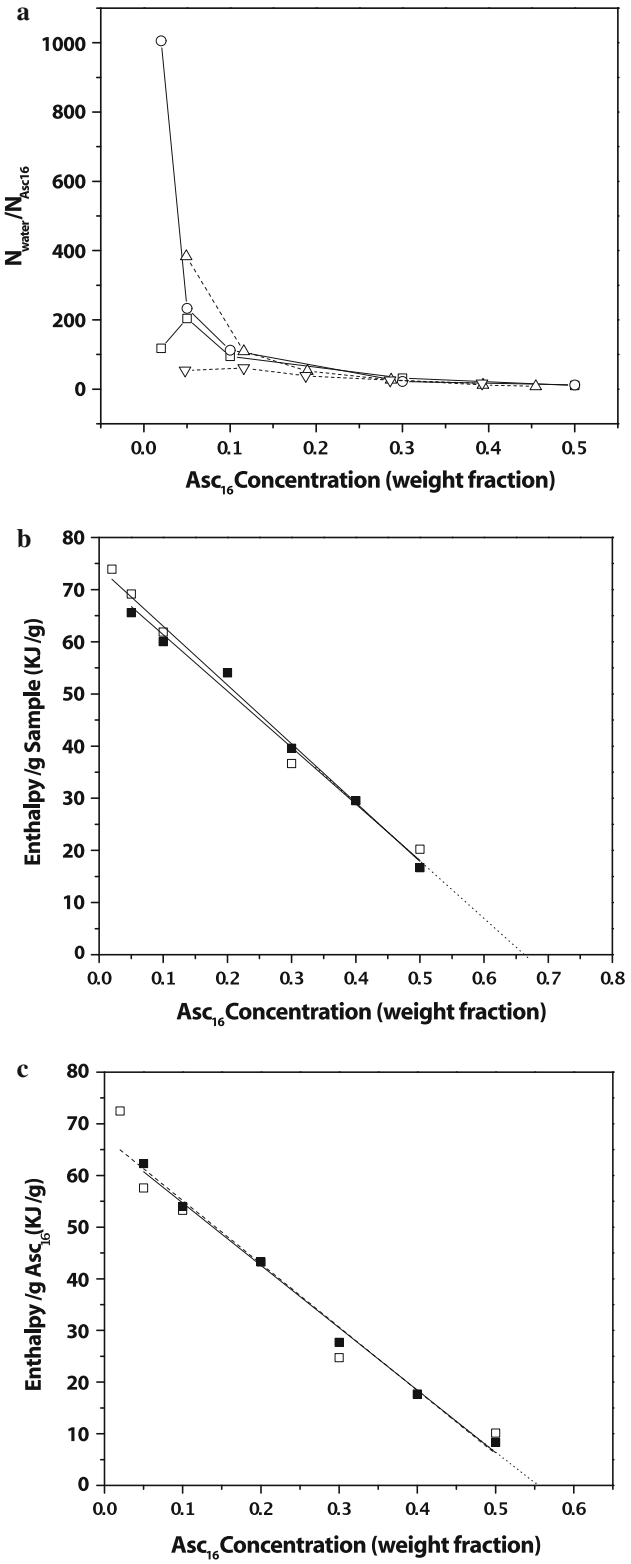


◀**Fig. 3** **a** Number of water molecules/surfactant: Δ bulk water in $Asc_{16}$-water, ∇ surface water in $Asc_{16}$-water, *open circles* bulk water in CpG-ODN/OVA/$Asc_{16}$-dextrose solution, *unfilled squares* surface water in CpG-ODN/OVA/$Asc_{16}$-dextrose solution. **b** Enthalpy per gram of sample *vs* $Asc_{16}$ weight fraction *unfilled squares* CpG-ODN/OVA/$Asc_{16}$-water, *filled squares* $Asc_{16}$-water. Linear fit of CpG-ODN/OVA/$Asc_{16}$-water (*dashed line*), and linear fit of $Asc_{16}$-water (*solid line*). **c** Enthalpy per gram of $Asc_{16}$ *vs* $Asc_{16}$ weight fraction *unfilled squares* CpG-ODN/OVA/$Asc_{16}$-water, *filled squares* $Asc_{16}$-water. Linear fit of CpG-ODN/OVA/$Asc_{16}$-water (*dashed line*), and linear fit of $Asc_{16}$-water (*solid line*)

the enthalpy per gram of sample is plotted, the system has no free water, and all the water belongs to the first hydration shell at $C = 0.667 \pm 0.007$ weight fraction which correspond to a hydration number of $11.5 \pm 1.3$ water molecules per $Asc_{16}$ molecule. These two values ($C = 0.667 \pm 0.007$ and $C = 0.55 \pm 0.005$ weight fraction) were estimated by fitting the curve.

Regarding the melting transition of water, it might be noticed that it is actually represented by two peaks. These peaks were separated into Gaussian components, which allow to determinate the beginning of the melting point and the respective enthalpies. Besides, the second hydration layer for $Asc_{16}$-water system involves around 50–60 water molecules/surfactant, directly connected to those located in the first hydration layer. This last layer could be affected by the presence of the polar head-groups resulting on a different melting peak in comparison with that of bulk water.

In the present work, with CpG-ODN/OVA/$Asc_{16}$-dextrose system, the overall water fusion peak disappeared at $0.671 \pm 0.009$ weight fraction of $Asc_{16}$ which corresponds to $11.2 \pm 1.2$ water molecules/$Asc_{16}$ molecule (Fig. 3b). This means that modifying the solvent (5 % dextrose solution instead of water) and the presence of hydrophilic compounds (CpG-ODN and OVA) do not disturb the lamellar arrangement reported before for $Asc_{16}$-water system. As seen in Fig. 3b, there is no difference between the extrapolated intersection point with $x$ axis (weight fraction Asc16) of CpG-ODN/OVA/$Asc_{16}$-dextrose solution and $Asc_{16}$-water systems. These results confirm that the first hydration layer had not been modified compared to the first hydration layer reported for $Asc_{16}$-water system. However, in the current study we observed that bulk water and second hydration water changed. For this system, the second hydration shell at 0.05 weight fraction shifts from ∼50 to ∼200 water molecules per $Asc_{16}$ molecule (Fig. 3a). These results were obtained by establishing the relation between the enthalpies of the different species of water related to the surfactant amount. The increased number of water molecules in this shell compared to $Asc_{16}$-water system is probably due to both hydrophilic compounds (CpG-ODN and OVA) being located in this second water layer between the lamellar phase layers, with all their –OH groups able to develop hydrogen bonds which could keep more water molecules in this location. The opposite

effect is observed at this concentration (0.05 weight fraction) when free water molecules of these two systems are considered. The number of water molecules shifts from ~386 ($Asc_{16}$-water system) to ~237 (CpG-ODN/OVA/$Asc_{16}$-dextrose system) per molecule of $Asc_{16}$ and this behavior could be related to the presence of hydrophilic compounds which increase the second hydration layer and in consequence, decreases the free (available) water molecules in the sample. When the concentration of $Asc_{16}$ is higher, this effect is less marked. Thus, if we consider the sum of molecules of water of both types in each system is possible to notice that the result is almost the same (~486 for the $Asc_{16}$-water system and 437 for the CpG-ODN/OVA/$Asc_{16}$-dextrose system) and only the distribution/proportions are different possibly due to the presence of a hydrophilic compound located in the second hydration layer.

It is important to note that the surface is formed by the first and the second hydration layers, and since the first one is not changed by the presence of hydrophilic compounds, the modification may be produced only inside the second hydration layer.

## FT-IR Analysis

In order to confirm the results obtained above, an infrared spectroscopy (FT-IR) analysis was carried out. Figure 4 shows IR spectra obtained from CpG-ODN/OVA loaded coagels at four representatives $Asc_{16}$ concentrations (0.1, 0.3, 0.5 and 0.7 weight fraction) in order to cover all the concentration range and extend the analysis to the entire phase diagram.

In the spectra, two bands at 3500 and 3000 $cm^{-1}$ are assigned to the oxygen-hydrogen stretching vibration. The sharp band at 3375 $cm^{-1}$ is labelled *C* and the second one, a broad band at around 3100-3300 $cm^{-1}$ was labelled B. The intensity of both bands increases by increasing the sample concentrations; nevertheless, band C keeps its position and B undergoes a shift to lower wavenumber values. The increase in intensities is due to the increased contribution of stretching modes of water and the shift in band B is due to the interaction between water and the -OH groups of the compound, which increases the association. In this sense, band B could be attributed to intermolecular bonds which increase with the concentration of $Asc_{16}$ and therefore, the number of water molecules. However, the shift of this band could be attributed to shorter and stronger bonds among the -OH groups of the superficial water which are exposed outside the crystal lattice forming aggregates with $Asc_{16}$ molecules when its concentration increase. The band at 1625 $cm^{-1}$, labelled A, is assigned to the deformation vibration of the -OH bond of water molecules in the sample, and thus, its intensity increases with the concentration of $Asc_{16}$, and therefore, the water content in the sample [42, 43]. The results obtained by FT-IR, allowed us to confirm that water behavior changes with $Asc_{16}$ concentrations; thus, when the concentration of $Asc_{16}$ in the system increases, the proportion of free water decreases. This result is in good accord with those obtained by DSC (Fig. 2). The increased intensity in band C is shown in Fig. 4 and confirms that once the amount of $Asc_{16}$ is increased, more bound water is found in the system, related to the surfactant polar heads. Notice that this increase could be visualized by FT-IR spectroscopy, while it is not possible to be detected by DSC, since the $Asc_{16}$/water ratio remains unchanged.

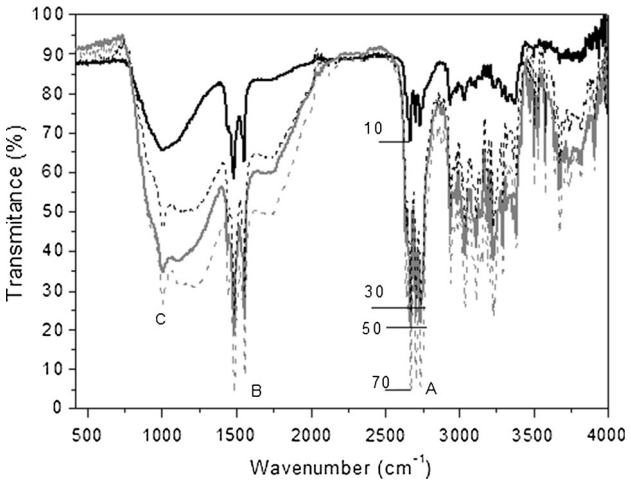


**Fig. 4** Infrared spectra. CpG-ODN/OVA/$Asc_{16}$ coagels. The concentrations and ratio CpG-ODN/OVA were kept constant and the concentration of $Asc_{16}$ in each sample was: 0.1, 0.3, 0.5 and 0.7 weight fraction

## Microscopic Analysis

In Fig. 5a, the photograph of 0.1 weight fraction of $Asc_{16}$ in water sample was taken while the sample was heated until 75 °C and myelin figures were observed (see bottom of the picture). This texture is characteristic of lamellar liquid crystals, as it was described by Benedini *et al.* [3]. The picture in Fig. 5b, also shows a texture of laminar liquid crystal characterized by the presence of oily streaks. Figure 5c shows light oily streaks from CpG-ODN/$Asc_{16}$ 0.1 weight fraction in dextrose solution system at 75 °C and in Fig. 5d we could see the same pattern even with the intercalation of 1$\lambda$ retardation plate. In these pictures (a, b, c, d) the effect of changing the solution, and the addition of CpG-ODN/OVA were compared. Indeed, the pictures do not show a phase perturbation at this concentration (0.1 weight fraction $Asc_{16}$). When the concentration of the samples was below the transition point between solid and lamellar liquid crystal, an isotropic solution and crystals

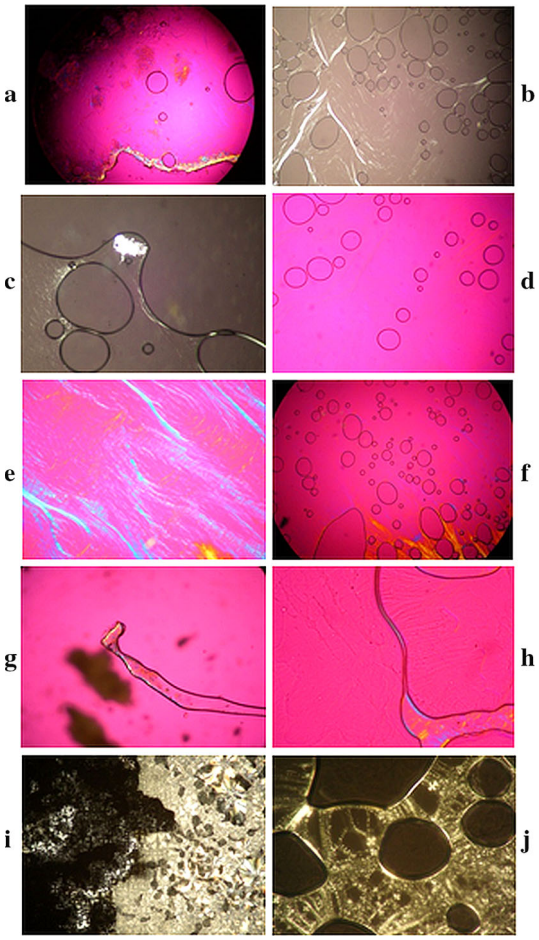


**Fig. 5** Photomicrographs with crossed polarizers (×100). **a** $Asc_{16}$ 0.1 weight fraction in water at 75 °C, myelin figures growing in an isotropic matrix (*bottom*), 1$\lambda$ retardation plate intercalated. **b** $Asc_{16}$ 0.1 weight fraction in dextrose solution at 75 °C, oily streaks can be observed. **c** CpG-ODN/$Asc_{16}$ 0.1 weight fraction in dextrose solution at 75 °C, light oily streaks appears. **d** CpG-ODN/OVA/$Asc_{16}$ 0.1 weight fraction in dextrose solution at 75 °C, 1$\lambda$ retardation plate intercalated and the presence of light oily streaks. **e** $Asc_{16}$ 0.3 weight fraction in water at 75 °C, 1$\lambda$ retardation plate intercalated, oily streaks are observed. **f** CpG-ODN/OVA/$Asc_{16}$ 0.3 weight fraction in dextrose solution at 75 °C, 1$\lambda$ retardation plate intercalated. At top oily streaks, at *bottom*, gel phase. **g** $Asc_{16}$ 0.5 weight fraction in water at 80 °C, 1$\lambda$ retardation plate intercalated, cubic liquid crystals are observed. **h** CpG-ODN/OVA/$Asc_{16}$ 0.5 weight fraction in dextrose solution at 75 °C, 1$\lambda$ retardation plate intercalated, liquid crystal phase is observed. **i** $Asc_{16}$ 0.7 weight fraction in water at 75 °C: on the right Maltese crosses and on the left gel phase. **j** CpG-ODN/OVA/$Asc_{16}$ 0.7 weight fraction in dextrose solution at 75 °C: Maltese crosses and oily streaks are observed

appeared. However, when the samples were heated above the transition point, a lamellar liquid crystal appeared. As it was seen in Fig. 2, the transition point for $Asc_{16}$-water systems, at concentrations below to 0.45 weight fraction was 62.5 °C, and it was not disturbed by the presence of CpG-ODN or OVA.

Figure 5e shows the $Asc_{16}$ 0.3 weight fraction in a water system at 75 °C with 1λ retardation plate intercalated. Here, oily streaks disclosed a lamellar liquid crystal. This behavior was also reported before [3] for all concentrations below 0.45 weight fraction in $Asc_{16}$-water system. Figure 5f shows the CpG-ODN/OVA/$Asc_{16}$ 0.3 weight fraction in a dextrose solution system at 75 °C, with 1$\lambda$ retardation plate intercalated. In this case, the temperature is not homogeneous; therefore, at the top of the picture oily streaks are present. These textures are clearly due to the low concentration of $Asc_{16}$ resulting on a low concentration of laminar liquid crystals. At the bottom of this picture, the gel phase appears due to a decrease in temperature below the phase transition temperature. Furthermore, no modifications in textures are displayed at the analyzed concentration and temperature. In Fig. 5g, a cubic liquid crystal is shown corresponding to $Asc_{16}$ 0.5 weight fraction in water at 90 °C and with 1λ retardation plate intercalated. This phase was also described in Ref. [3]. It is important to stress that this event occurs almost in absence of free water, thus, the isotropic phase that is shown in this picture cannot be produced by the presence of aqueous solution, but it should be a cubic liquid crystal. The cubic phase occurs in small domains of concentration and temperature, and appears as a rigid gel. The picture in Fig. 5h describes the CpG-ODN/OVA/$Asc_{16}$ 0.5 weight fraction in a dextrose solution system at 75 °C with a 1$\lambda$ retardation plate intercalated. Here a cubic liquid crystal is also present; however, its formation temperature is lower than in the $Asc_{16}$-water system. This difference could be related to the zone of the phase diagram, which corresponds to a transition zone where bulk water has disappeared; therefore, the effect of CpG-ODN/OVA in the second hydration layer would be more important and the cubic liquid crystal begins to appear. Figure 5i shows the $Asc_{16}$ 0.7 weight fraction in water at 75 °C, and in that case Maltese crosses are observed on the right and a gel phase on the left side. The occurrence of these two phases is related to a non-homogenous temperature in the sample. The Maltese crosses correspond to a lamellar liquid crystal texture which is found at higher temperature than the gel phase. This last phase appears when the sample is cooled after the formation of lamellar liquid crystals at high temperature. In this viscous systems the growth of solid crystals after liquid crystal formation is conditioned by the kinetics; furthermore, on cooling, this gel phase turns into a coagel and later into solid crystals. This effect has been described by Benedini *et al.* [3]. Finally, in Fig. 5j, the same system that Fig. 5i but in dextrose solution, Maltese crosses and oily streaks are observed. These structures are typical of lamellar liquid crystal and their aspect is in concordance with the previous figure, showing that the presence of CpG-ODN/OVA does not disturb the formation of mesophases.

## The Phase Diagram

Figure 6a, b show the phase diagrams of $Asc_{16}$-water [3] and CpG-ODN/OVA/$Asc_{16}$-dextrose solution respectively, obtained by a combination of DSC measurements, thermodynamic calculation, and polarizing microscopy.

In the low concentration region and below 60 °C, both systems are composed of a mixture of hydrated crystals in an isotropic liquid. As temperature rises, two-phase areas appear around 60–70 °C (depending on the concentration), resulting in a lamellar mesophase with a classical low-birefringent and smooth oiled streaks (compared Fig. 5b, $Asc_{16}$ in water; and 5.e, CpG-ODN/OVA/$Asc_{16}$ in dextrose solution). In a system with a 0.1 weight fraction of $Asc_{16}$-water, the transition temperature described in previous reports is 62.5 °C [1, 3]. Due to the differences in the texture of numerous concentrated liquid crystals, this stage has been called a low concentration lamellar mesophase as it was designated in both diagrams. The increase in temperature in systems with no bulk water ($C \geq 0.48$ weight fraction), provokes an abrupt increase in the transition temperature (starting from ~60 to ~80 °C). Furthermore, rather than noticing a singular progression from hydrated crystals to lamellar mesophase, two events can be registered: the passage from hydrated crystals toward a cubic viscoisotropic (V) mesophase (between 80 and 88 °C) and from a cubic mesophase into a high concentration lamellar liquid crystal (94–104 °C). This last mesophase shows more birefringent and rougher oily streaks arrangement. A difference between both phase diagrams was observed at $Asc_{16}$ concentrations higher than 0.5 weight fraction. On one hand, $Asc_{16}$-water system shows a high concentration lamellar liquid crystal with a more birefringent and coarse oily streaks texture compared to the lower concentrations. On the other hand, the system with CpG-ODN/OVA/$Asc_{16}$ dextrose solution displays a coexistence of both lamellar liquid crystals with coarse oily streaks texture and smooth oily streaks (see Fig. 5h).

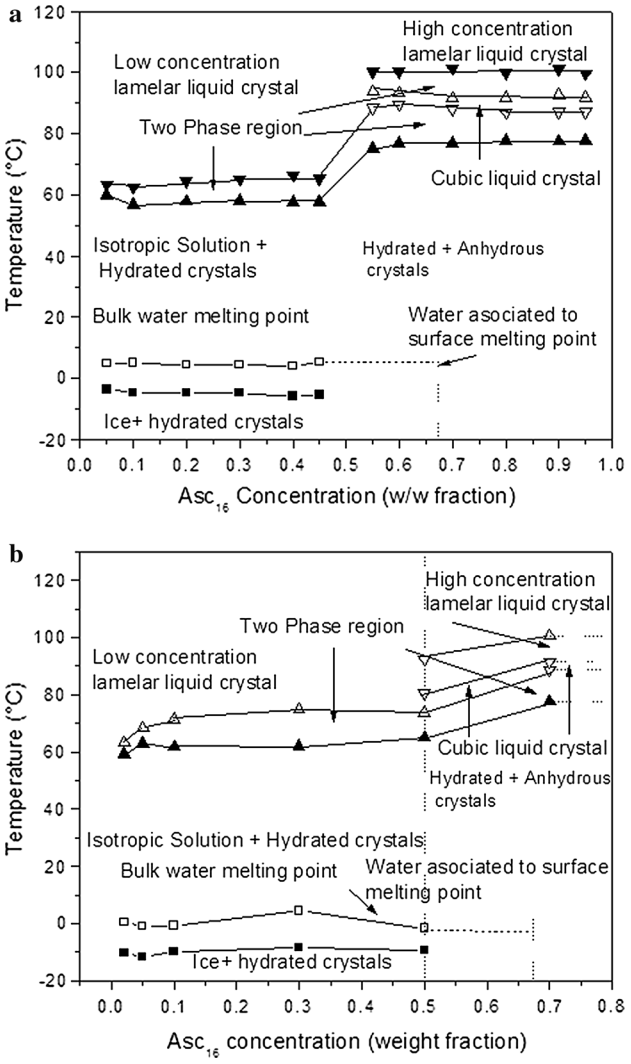


**Fig. 6** **a** Phase diagram of $Asc_{16}$ in water extracted from Benedini *et al.* [3]. **b** Phase diagram of CpG-ODN/OVA/$Asc_{16}$ in dextrose solution system

CpG-ODN/OVA/$Asc_{16}$ dextrose solution system shows on cooling the appearance of a gel phase from the lamellar liquid crystal. As it was seen in Fig. 5e, the coexistence of oil streaks typical of lamellar liquid crystals with coarse structures typical of the gel phase was due to a relatively rapid cooling (i.e., the temperature in the sample was not homogeneous). When the system was left at room temperature, it slowly turned into a coagel, i.e., a mixture of isotropic solution and microcrystals.

As it was reported by Caboi *et al.* [44], the addition of compounds without amphiphilic behavior into liquid crystals systems in concentrations lower than 12 %, does not disturb the liquid crystal structures. In the system studied here this effect was also observed. Furthermore, Murgia *et al.* [45] reported that hydrophilic additives, do not alter the formation of the phases and no changes in the local order are presented.

In conclusion, for the systems composed by $Asc_{16}$ coagels in dextrose solution, it was confirmed that water is in three different states and the nature of the mesophases formed is affected by temperature. These results are consistent with those described for the $Asc_{16}$-water system in which changes were not observed due to the presence of saccharides [39]. In addition, after loading CpG-ODN and OVA into coagels there was no formation of new mesophases. Moreover, the differences found in the free water and mainly in the secondary hydration layer, could confirm that the studied compounds are situated in the aqueous domain, and in direct contact with the first hydration shell. These observations allow us to infer that the oligonucleotide (CpG-ODN) and the protein (OVA) are located in

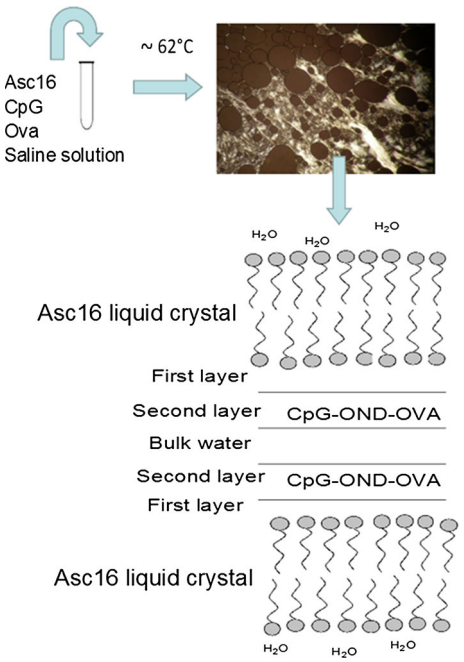


**Fig. 7** Schematic picture of the microscopic structural model. The oligonucleotide (CpG-ODN) and the protein (OVA) are located in the aqueous environment inside the coagel

the aqueous environment inside the coagel. A schematic picture of the microscopic structural model proposed for this system is shown in Fig. 7. Nevertheless, this environment is also surrounded and confined by numerous hydrocarbon layers which could prolong the release of these compounds, a desirable characteristic for an ideal oligonucleotide delivery system.

When comparing the charged and uncharged system it seems that an increase of $Asc_{16}$ concentration generates a systematic increase of birefringence in both cases. Although this trend is the same for both systems, in loaded liquid crystals this modification is observed at low concentrations, in which the birefringence is less intense.

The construction and analysis of the phase diagrams performed with $Asc_{16}$ and hydrophilic additives could be a useful tool to design systems with the same matrix and other water-soluble components.

**Acknowledgments** The authors would like to thank Dra. Olga Pieroni, (Organic Chemistry Laboratory-Chemistry department from UNS.INQUISUR-CONICET Bahia Blanca, Argentina) for assistance with the IR analysis. G. Ullio Gamboa thanks the Consejo Nacional de Investigaciones Científicas y Técnicas (CONICET) for a research fellowship. This work was supported by the grants SECyT-UNC. Res. 162/12 and PID CONICET No. 11220090100673 and a grant of the Universidad Nacional del Sur. LAB, and DAA are researchers of CONICET.

**Compliance with Ethical Standards**

**Conflict of interest** The authors declare that they have no conflict of interest.

## References

1. Palma S, Lo Nostro P, Manzo R, Allemandi D (2002) Evaluation of the surfactant properties of ascorbyl palmitate sodium salt. Eur J Pharm Sci 16:37–43
2. Palma S, Manzo R, Allemandi D, Fratoni L, Lo Nostro P (2002) Solubilization of hydrophobic drugs in octanoyl-6-*O*-ascorbic acid micellar dispersions. Langmuir 18:1810–1816
3. Benedini L, Schulz E, Messina P, Palma S, Allemandi D, Schulz P (2011) The ascorbyl palmitate-water system: phase diagram and state of water. Colloids Surf A Physicochem Eng Aspects 375:178–185
4. Palma S, Ullio Gamboa G, Allemandi D (2013) Vitamin C based nanostructures: potential utility in ocular and transdermal therapy. J Biomater Tiss Eng 3:61–69
5. Ambrosi M, Lo Nostro P, Fratoni L, Dei L, Ninham BW, Palma S, Manzo R, Allemandi D, Baglioni P (2004) Water of hydration in coagels. Phys Chem Chem Phys 6:1401–1407
6. Palma S, Manzo R, Allemandi D, Fratoni L, Lo Nostro P (2003) Drugs solubilization in ascorbyl-decanoate micellar solutions. Colloids Surf A Physicochem Eng Aspects 212:163–173
7. Capuzzi G, Lo Nostro P, Kulkarni K, Fernandez J, Vincieri F (1996) Interactions of 6-*O*-stearoylascorbic acid and vitamin K1 in mixed Langmuir films at the gas–water interface. Langmuir 12:5413–5418
8. Capuzzi G, Lo Nostro P, Kulkarni K, Fernandez J (1996) Mixtures of stearoyl-6-*O*-ascorbic acid and -tocopherol: a monolayer study at the gas/water interface. Langmuir 12:3957–3963
9. Capuzzi G, Kulkarni G, Fernandez J, Vincieri J, Lo Nostro P (1997) Mixture of ascorbyl-stearate and vitamin D3: a monolayer study at the gas–water interface. J Colloid Interface Sci 186:271–279
10. Tartara I, Quinteros D, Saino V, Allemandi D, Palma S (2012) Improvement of acetazolamide ocular permeation using ascorbyl laurate nanostrucures as drug delivery systems. J Ocul Pharmacol Ther 28:102–109
11. Saino V, Monti D, Burgalassi S, Tampucci S, Palma S, Allemandi D, Chetoni P (2010) Optimization of skin permeation and distribution of ibuprofen by using nanostructures (coagels) based on alkyl vitamin C derivatives. Eur J Pharm Biopharm 76:443–449
12. Palma S, Maletto B, Lo Nostro P, Manzo R, Pistoresi-Palencia M, Allemandi D (2006) Potential use of ascorbic acid–based surfactants as skin penetration enhancers. Drug Dev Ind Pharm 32:821–827
13. Rasia M, Spengler M, Palma S, Manzo R, Lo Nostro P, Allemandi D (2011) Effect of ascorbic acid based amphiphiles on human erythrocytes membrane. Clin Hemorheol Microcirc 36:133–140
14. Pulendran B, Ahmed R (2011) Immunological mechanisms of vaccination. Nat Immunol 12:509–517
15. Hanagata N (2012) Structure-dependent immunostimulatory effect of CpG oligodeoxynucleotides and their delivery system. Int J Nanomed 7:2181–2195
16. Navarro G, Maiwald G, Haase R, Rogach A, Wagner E, Tros de Ilarduya C, Ogris M (2010) Low generation PAMAM dendrimer and CpG free plasmids allow targeted and extended transgene expression in tumors after systemic delivery. J Controll Rel 146:99–105
17. Gramzinski R, Doolan D, Sedegah M, Davis H, Krieg A, Hoffman S (2001) Interleukin-12- and gamma interferon-dependent protection against malaria conferred by CpG oligodeoxynucleotide in mice. Infect Immun 69:1643–1649
18. Rees D, Gates A, Green M, Eastaugh L, Lukaszewski R, Griffin K, Krieg AM, Titball RW (2005) CpG-DNA protects against a

lethal orthopoxvirus infection in a murine model. Antivir Res 65:87–95
19. Mutwiri G, van DrunenLittel-van den Hurk S, Babiuk L (2009) Safety of CpG oligodeoxynucleotides in veterinary species. Adv Drug Deliv Rev 61:226–232
20. Krieg A (2006) Therapeutic potential of toll-like receptor 9 activation. Nat Rev Drug Discov 5:471–484
21. Mutwiri G, Nichani A, Babiuk S, Babiuk L (2004) Strategies for enhancing the immunostimulatory effects of CpG oligodeoxynucleotides. J Control Release 97:1–17
22. Mueller M, Reichardt W, Koerner J, Groettrup M (2012) Coencapsulation of tumor lysate and CpG-ODN in PLGA-microspheres enables successful immunotherapy of prostate carcinoma in TRAMP mice. J Control Release 162:159–166
23. Kwong B, Liu H, Irvine DJ (2011) Induction of potent anti-tumor responses while eliminating systemic side effects via liposome-anchored combinatorial immunotherapy. Biomaterials 32:5134–5147
24. Klier J, Fuchs S, May A, Schillinger U, Plank C, Winter G, Gehlen H, Coester C (2012) A nebulized gelatin nanoparticle-based CpG formulation is effective in immunotherapy of allergic horses. Pharm Res 29:1650–1657
25. Zhou S, Hashida Y, Kawakami S, Mihara J, Umeyama T, Imahori H, Murakami T, Yamashita F, Hashida M (2014) Preparation of immunostimulatory single-walled carbon nanotube/CpG DNA complexes and evaluation of their potential in cancer immunotherapy. Int J Pharm 471:214–223
26. Choksakulnimitr S, Masuda S, Tokuda H, Takakura Y, Hashida M (1995) In vitro cytotoxicity of macromolecules in different cell-culture systems. J Control Release 34:233–241
27. Rattanakiat S, Nishikawa SM, Funabashi H, Luo D, Takakura Y (2009) The assembly of a short linear natural cytosine-phosphate-guanine DNA into dendritic structures and its effect on immunostimulatory activity. Biomaterials 30:5701–5706
28. Klinman D, Barnhart K, Conover J (1999) CpG motifs as immune adjuvants. Vaccine. 17:19–25
29. Klinman D (2006) Adjuvant activity of CpG oligodeoxynucleotides. Int Rev Immunol 25:135–154
30. Xie H, Gursel I, Ivins B, Singh M, O'Hagan D, Ulmer J, Klindman D (2005) CpG oligodeoxynucleotides adsorbed onto polylactide-co-glycolide microparticles improve the immunogenicity and protective activity of the licensed anthrax vaccine. Infect Immun 73:828–833
31. Erikci E, Gursel M, Gursel I (2011) Differential immune activation following encapsulation of immunostimulatory CpG oligodeoxynucleotide in nanoliposomes. Biomaterials 32:1715–1723
32. Fischer S, Schlosser E, Mueller M, Csaba N, Merkle HP, Groettrup M, Gander B (2009) Concomitant delivery of a CTL-restricted peptide antigen and CpG ODN by PLGA microparticles induces cellular immune response. J Drug Target 17(8):652–661
33. McCluskie MJ, Weeratna RD, Evans DM, Makinen S, Drane D, Davis HL (2013) CpG ODN and ISCOMATRIX adjuvant: a synergistic adjuvant combination inducing strong T-cell IFN-gamma responses. Biomed Res Int 2013:636847
34. Sánchez Vallecillo M, Ullio Gamboa G, Palma S, Harman M, Chiodetti M, Morón G, Pstoresi C, Maletto B (2014) Adjuvant activity of CpG-ODN formulated as a liquid crystal. Biomaterials 35:2529–2542
35. Schulz PC (2006) Water structure at surfactant microstructures and biological interfaces. In: Somasundaran P, Hubbard A (eds) Encyclopedia of surface and colloid science, New York, pp 6562–6577
36. Maletto B, Ropolo A, Moron V, Pistoresi-Palencia MC (2002) CpG-DNA stimulates cellular and humoral immunity and promotes Th1 differentiation in aged BALB/c mice. JLB 72:447–454
37. Maletto B, Ropolo A, Liscovsky M, Alignani D, Glocker M, Pistoresi-Palencia M (2005) CpG oligodeoxinucleotides functions as an effective adjuvant in aged BALB/c mice. Clin Immunol 117:251–261
38. Connors K, Amidon G, Stella I (1986) Chemical stability of pharmaceuticals, Wiley-Interscience, New York
39. Rowe RC, Sheskey PJ, Cook W, Fenton ME (2012) Handbook of pharmaceutical excipients. American Pharmaceutical Association, Washington DC
40. Lo Nostro P, Ninham BW, Fratoni L, Palma S, Manzo RH, Allemandi D, Baglioni P (2003) Effect of water structure on the formation of coagels from ascorbylalkanoates. Langmuir 19:3222–3228
41. Schulz PC, Soltero-Martínez JFA, Puig JE (2001) DSC analysis of surfactant-based microstructures. In: Garti N (ed) Thermal behavior of dispersed systems. New York, pp 121–181
42. Herrera-Gómez A, Velázquez-Cruz G, Martín-Polo M (2001) Analysis of the water bound to a polymer matrix by infrared spectroscopy. J Appl Phys 89:5431–5437
43. Zhou G, Li G, Chen W (2002) Fourier transform infrared investigation on water states and the conformations of aerosol-OT in reverse microemulsions. Langmuir 18:4566–4571
44. Caboi F, Amico G, Pitzalis P, Monduzzi M, Nylander T, Larsson K (2001) Addition of hydrophilic and lipophilic compounds of biological relevance to the monoolein/water system. I. Phase behaviour. Chem Phys Lipids 109:47–62
45. Murgia S, Caboi F, Monduzzi M (2001) Addition of hydrophilic and lipophilic compounds of biological relevance to the monoolein:water system II—$^{13}$C NMR relaxation study. Chem Phys Lipids 110:11–17

**Gabriela V. Ullio Gamboa** (Ph.D. in Chemistry, Pharmacist) is a research scientist and member of the Pharmaceutical Research Team (UNITEFA) of the National Scientific and Technical Research Council (CONICET) in Córdoba, Argentina. UNITEFA aims to develop new pharmaceutical platforms for drug delivery. Dr. Ullio Gamboás research is based on nanotechnology and nanomedicines, and encompasses both drug targeting and the development of encapsulation methods for active ingredients.

**Luciano A. Benedini** (Ph.D. in Chemistry, Pharmacist) is an Assistant Scientific Researcher of the Chemical Research Team (INQUISUR) of the National Scientific and Technical Research Council (CONICET) in Bahia Blanca, Argentina. INQUISUR aims to develop and characterize nanostructured materials, colloids and interfaces. His research is focussed on the antioxidant nano-particles applicable to calcified tissue disorders.

**Pablo C. Schulz** (Ph.D. in Chemistry, Biochemist) is a lecturer at the Universidad Nacional del Sur (UNS), in Bahía Blanca, Argentina, where he is an Honorary Professor. His research is focussed on the chemistry of interfaces and colloids fields, in particular concerning topics related to surfactants, their physicochemical properties (structures, phases, interaction with proteins and polyelectrolytes) and their application in food and analytical chemistry (emulsions, microemulsions, polymerization).

**Daniel A. Allemandi** (Ph.D. in Chemistry, Pharmacist) is a lecturer at the Faculty of Chemical Sciences, National University of Córdoba, Argentina. He is the Chief Director of the Pharmaceutical Research Team (UNITEFA) and also a Principal Scientific Researcher of the National Scientific and Technical Research Council (CONICET) in Córdoba, Argentina. His research is focussed on pharmaceutical technology, in particular nanoparticulate drug delivery systems, modified release and innovative drug delivery systems for ophthalmic administration.